

Computation of eigenfrequency sensitivities using Riesz projections for efficient optimization of nanophotonic resonators

Felix Binkowski¹, Fridtjof Betz¹, Martin Hammerschmidt², Philipp-Immanuel Schneider², Lin Zschiedrich² & Sven Burger^{1,2}✉

Resonances are omnipresent in physics and essential for the description of wave phenomena. We present an approach for computing eigenfrequency sensitivities of resonances. The theory is based on Riesz projections and the approach can be applied to compute partial derivatives of the complex eigenfrequencies of any resonance problem. Here, the method is derived for Maxwell's equations. Its numerical realization essentially relies on direct differentiation of scattering problems. We use a numerical implementation to demonstrate the performance of the approach compared to differentiation using finite differences. The method is applied for the efficient optimization of the quality factor of a nanophotonic resonator.

¹Zuse Institute Berlin, 14195 Berlin, Germany. ²JCMwave GmbH, 14050 Berlin, Germany. ✉email: burger@zib.de

Resonance phenomena are ubiquitous in nanophotonics and play an important role for tailoring light-matter interactions^{1,2}. They are exploited in, e.g., single-photon sources for quantum technology³, biosensors⁴, nanolasers⁵, or solar energy devices^{6,7}. All these applications rely on the highly localized electromagnetic field energies in the vicinity of the underlying nanoresonators⁸. A central figure of merit for the description of resonance effects is the quality (Q) factor, which quantifies, in the case of low-loss systems, the relation between stored and radiated field energies of the resonances⁹. Nanoresonators with low energy dissipation, i.e., with high Q -factors, have been proposed to improve the efficiencies of nanophotonic devices^{2,10}. For example, high- Q resonators can boost the brightness of quantum emitters, the sensitivity of sensors, or the emission processes in plasmonic lasers¹¹. Designing devices with numerical optimization is a time and cost-effective approach. The resonances are numerically computed by solving the source-free Maxwell's equations equipped with open boundary conditions¹². This yields non-Hermitian eigenproblems and the solutions are eigenmodes with complex-valued eigenfrequencies. In this context, the Q -factor is defined as the scaled ratio of the real and imaginary parts of the eigenfrequency.

Nanoresonators with high Q -factors have been theoretically presented, but fabrication of these resonators is a limiting task¹¹. The sensitivity analysis of eigenfrequencies can show a way to reduce the sensitivities of the Q -factors. This can support the nanofabrication processes. Furthermore, the sensitivity analysis of eigenfrequencies is essential for numerical simulation. For example, the numerical accuracies of the calculated eigenfrequencies are strongly influenced by the sensitivities of the eigenfrequencies when the systems are subject to small perturbations^{13,14}. In particular, for high- Q resonators, the accuracy requirements are demanding since the real and imaginary parts of the eigenfrequencies differ by several orders of magnitude. Sensitivities are also directly exploited in numerical optimization algorithms using gradients¹⁵, for gradient-enhanced surrogate modeling¹⁶, and for local sensitivity analyses¹⁷. The computation of eigenfrequency sensitivities is usually based on perturbation theory^{18,19}, where the sensitivity of the underlying operator, the left and the right eigenmodes, and a proper normalization of the eigenmodes are required. The solution of the perturbed systems, on the other hand, is not necessary. For resonance problems, left and right eigenmodes are in general not identical, which increases the computational effort, and normalization requires additional attention. There are specialized approaches that, e.g., exploit magnetic fields for extracting the left eigenmodes²⁰, introduce an adjoint system for computing sensitivities²¹, or that rely on internal and external electric fields at the boundaries of the nanoresonators²². It is also possible to completely omit the use of eigenmodes for sensitivity analysis²³. A further approach is the straightforward application of finite differences. However, this also includes the solution of the perturbed resonance problems, which increases the computational effort.

In this work, we present an approach for computing eigenfrequency sensitivities that completely avoids solving resonance problems. The approach is based on Riesz projections given by contour integrals in the complex frequency plane. The contour integrals are numerically accessed by solving Maxwell's equations with a source term enabling an efficient numerical realization using direct differentiation. The numerical experiments show a significant reduction in computational effort compared to applying finite differences. A Bayesian optimization algorithm with the incorporation of eigenfrequency sensitivities is used to optimize a resonator hosting a resonance with a high Q -factor.

Results

Theoretical background and numerical realization. We start with an introduction of the theoretical background on resonance phenomena occurring in nanophotonics. Based on this, Riesz projections for computing eigenfrequency sensitivities and an efficient approach for its numerical realization are presented.

Resonances in nanophotonics. In nanophotonics, in the steady-state regime, light-matter interactions can be described by the time-harmonic Maxwell's equations in second-order form,

$$\nabla \times \mu_0^{-1} \nabla \times \mathbf{E}(\mathbf{r}, \omega_0) - \omega_0^2 \epsilon(\mathbf{r}, \omega_0) \mathbf{E}(\mathbf{r}, \omega_0) = i\omega_0 \mathbf{J}(\mathbf{r}), \quad (1)$$

where $\mathbf{E}(\mathbf{r}, \omega_0) \in \mathbb{C}^3$ is the electric field, $\mathbf{r} \in \mathbb{R}^3$ is the position, $\omega_0 \in \mathbb{R}$ is the angular frequency, and $\mathbf{J}(\mathbf{r}) \in \mathbb{C}^3$ is the electric current density corresponding to a light source. In the optical regime, the permeability tensor $\mu(\mathbf{r}, \omega_0)$ typically equals the vacuum permeability μ_0 . The permittivity tensor $\epsilon(\mathbf{r}, \omega_0) = \epsilon_r(\mathbf{r}, \omega_0)\epsilon_0$, where $\epsilon_r(\mathbf{r}, \omega_0)$ is the relative permittivity and ϵ_0 the vacuum permittivity, describes the spatial distribution of material and the material dispersion. Solutions to Eq. (1) are called scattering solutions as light from a source is scattered by a material system.

Resonances are solutions to Eq. (1) without a source term, i.e., $\mathbf{J}(\mathbf{r}) = 0$, and with transparent boundary conditions. The boundary conditions lead to non-Hermitian eigenproblems, and, if material dispersion is also present, the eigenproblems become nonlinear. The electric field distribution of an eigenmode is denoted by $\tilde{\mathbf{E}}(\mathbf{r}) \in \mathbb{C}^3$ and the corresponding complex-valued eigenfrequency by $\tilde{\omega} \in \mathbb{C}$. The Q -factor of a resonance is defined by

$$Q = \frac{\text{Re}(\tilde{\omega})}{-2\text{Im}(\tilde{\omega})}$$

and describes its spectral confinement. In the limiting case of vanishing losses, this definition agrees with the energy definition, according to which the Q -factor quantifies the relation between stored and dissipated electromagnetic field energy of a resonance⁹.

In the following, a nanophotonic resonator supporting a resonance with a high Q -factor is investigated. We compute the eigenfrequency sensitivities with respect to various parameters to optimize the Q -factor of the nanoresonator. Figure 1 sketches the applied framework for an exemplary problem, a one-dimensional resonator defined by layers with different permittivities. Changes δp of the parameter p lead to changes in the eigenmode $\tilde{\mathbf{E}}$ and in the corresponding eigenfrequency $\tilde{\omega}$, which describes the sensitivity of $\tilde{\mathbf{E}}$ and $\tilde{\omega}$ with respect to the parameter p . To compute the eigenfrequency sensitivity, we introduce a contour-integral-based approach using Riesz projections, where physical observables are extracted from scattering problems. Solving the scattering problems, which are linear systems, can be regarded as a blackbox^{24,25}.

Riesz projections for eigenfrequency sensitivities. To derive a Riesz-projection-based approach for computing eigenfrequency sensitivities, which are the partial derivatives of the eigenfrequency, we consider the electric field $\mathbf{E}(\mathbf{r}, \omega_0 \in \mathbb{R})$ as a solution of Eq. (1) and $\mathbf{E}(\mathbf{r}, \omega \in \mathbb{C})$ as an analytical continuation of $\mathbf{E}(\mathbf{r}, \omega_0)$ into the complex frequency plane. The field $\mathbf{E}(\mathbf{r}, \omega)$ is a meromorphic function with resonance poles at the eigenfrequencies. To simplify the notation, we omit the spatial and frequency dependency of the electric field and write $\tilde{\mathbf{E}}$ when we mean $\mathbf{E}(\mathbf{r}, \omega)$.

Let $\mathcal{L}(\tilde{\mathbf{E}})$ be a physical observable, where $\mathcal{L}: \mathbb{C}^3 \rightarrow \mathbb{C}$ is a linear functional, and \tilde{C} be a contour enclosing the pole $\tilde{\omega}$ of the order m and no other poles. Then, the Laurent expansion of $\mathcal{L}(\tilde{\mathbf{E}})$

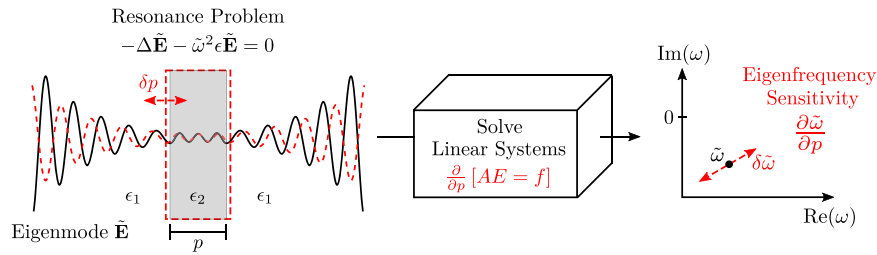


Fig. 1 Schematic representation of computing eigenfrequency sensitivities of a resonator using contour integration. The system is defined by layers with different permittivities ϵ_1 and ϵ_2 and is described by the one-dimensional Helmholtz equation $-\Delta \tilde{\mathbf{E}} - \tilde{\omega}^2 \epsilon \tilde{\mathbf{E}} = 0$. A solution to the resonance problem is given by the eigenmode $\tilde{\mathbf{E}}$ and the corresponding complex-valued eigenfrequency $\tilde{\omega} \in \mathbb{C}$. The real part of the electric field of the eigenmode is sketched with the solid black curve. A perturbation δp of the middle layer width p leads to a perturbed electric field, represented by the dashed red curve, and to a perturbation $\delta \tilde{\omega}$ of the eigenfrequency. Computing contour integrals by solving linear systems $A\mathbf{E} = \mathbf{f}$ and $\partial/\partial p[A\mathbf{E} = \mathbf{f}]$ in the complex frequency plane yields the eigenfrequency sensitivity $\partial \tilde{\omega} / \partial p$. Solving the linear systems is considered as a blackbox.

about $\tilde{\omega}$ is given by

$$\mathcal{L}(\mathbf{E}) = \sum_{k=-m}^{\infty} a_k(\omega - \tilde{\omega})^k, \text{ where} \quad (2)$$

$$a_k(\tilde{\omega}) = \frac{1}{2\pi i} \oint_{\tilde{C}} \frac{\mathcal{L}(\mathbf{E}(\omega))}{(\omega - \tilde{\omega})^{k+1}} d\omega \in \mathbb{C}.$$

The coefficient $a_{-1}(\tilde{\omega})$ is the so-called residue of $\mathcal{L}(\mathbf{E})$ at $\tilde{\omega}$. Using Eq. (2) with the assumption that $\tilde{\omega}$ has the order $m = 1$ and applying Cauchy's integral formula yield

$$\oint_{\tilde{C}} \omega \mathcal{L}(\mathbf{E}) d\omega = \oint_{\tilde{C}} \frac{\omega}{\omega - \tilde{\omega}} a_{-1}(\tilde{\omega}) d\omega = \tilde{\omega} \oint_{\tilde{C}} \mathcal{L}(\mathbf{E}) d\omega,$$

where, due to the closed integral in the complex plane, the regular terms in the expansion vanish. With this, the eigenfrequency $\tilde{\omega}$ is given by

$$\tilde{\omega} = \frac{\oint_{\tilde{C}} \omega \mathcal{L}(\mathbf{E}) d\omega}{\oint_{\tilde{C}} \mathcal{L}(\mathbf{E}) d\omega}. \quad (3)$$

The contour integrals in this equation are essentially Riesz projections for $\mathcal{L}(\mathbf{E})$ and \tilde{C}^{24} . Partial differentiation with respect to a parameter p directly gives the desired expression for the eigenfrequency sensitivity,

$$\frac{\partial \tilde{\omega}}{\partial p} = \left(\frac{\partial u}{\partial p} v - u \frac{\partial v}{\partial p} \right) \frac{1}{v^2}, \text{ where} \quad (4)$$

$$u = \oint_{\tilde{C}} \omega \mathcal{L}(\mathbf{E}) d\omega, v = \oint_{\tilde{C}} \mathcal{L}(\mathbf{E}) d\omega,$$

$$\frac{\partial u}{\partial p} = \oint_{\tilde{C}} \omega \mathcal{L} \left(\frac{\partial \mathbf{E}}{\partial p} \right) d\omega, \frac{\partial v}{\partial p} = \oint_{\tilde{C}} \mathcal{L} \left(\frac{\partial \mathbf{E}}{\partial p} \right) d\omega.$$

For the interchangeability of integral and derivative, \mathbf{E} and $\partial \mathbf{E} / \partial p$ are assumed to be continuously differentiable with respect to the frequency ω and the parameter p . The eigenmode $\tilde{\mathbf{E}}$ and its sensitivity $\partial \tilde{\mathbf{E}} / \partial p$ can be represented by the contour integrals

$$\tilde{\mathbf{E}} = \oint_{\tilde{C}} \mathbf{E} d\omega \text{ and } \frac{\partial \tilde{\mathbf{E}}}{\partial p} = \oint_{\tilde{C}} \frac{\partial \mathbf{E}}{\partial p} d\omega,$$

respectively, which are Riesz projections applied to Maxwell's equations given by Eq. (1). This approach can be generalized for multiple eigenfrequencies inside a contour as well as for higher order poles; cf. Binkowski et al.²⁴. Note that Riesz projections can also be used to compute modal expansions of physical

observables, where scattering solutions are expanded into weighted sums of eigenmodes²⁶.

Numerical realization and direct differentiation. For the numerical realization of the presented approach, the finite element method (FEM) is applied. Scattering problems are solved by applying the solver JCMSUITE²⁷. The FEM discretization of Eq. (1) leads to the linear system of equations $A\mathbf{E} = \mathbf{f}$, where $A \in \mathbb{C}^{n \times n}$ is the system matrix, $\mathbf{E} \in \mathbb{C}^n$ is the scattered electric field in a finite-dimensional FEM basis, and $\mathbf{f} \in \mathbb{C}^n$ contains the source term. The solver employs adaptive meshing and higher order polynomial ansatz functions. In all subsequent simulations, it is ensured that sufficient accuracies are achieved with respect to the FEM discretization parameters. Note that also other methods can be used for numerical discretization. In the field of nanophotonics, common approaches are, e.g., the finite-difference time-domain method, the Fourier modal method, or the boundary element method^{12,28}.

In order to calculate eigenfrequencies $\tilde{\omega}$ and their sensitivities $\partial \tilde{\omega} / \partial p_i$ with respect to parameters p_i , the electric fields \mathbf{E} and their sensitivities $\partial \mathbf{E} / \partial p_i$ are computed for complex frequencies $\omega \in \mathbb{C}$ on the contours given in Eqs. (3) and (4). For the calculation of $\partial \mathbf{E} / \partial p_i$, we apply an approach based on directly using the FEM system matrix^{29,30}. With this direct differentiation method, the sensitivities of scattering solutions can be computed by

$$\frac{\partial \mathbf{E}}{\partial p_i} = A^{-1} \left(\frac{\partial \mathbf{f}}{\partial p_i} - \frac{\partial A}{\partial p_i} \mathbf{E} \right). \quad (5)$$

In a first step, instead of directly computing A^{-1} , an LU -decomposition of A , which can be seen as the matrix variant of Gaussian elimination, is computed to efficiently solve the linear system $A\mathbf{E} = \mathbf{f}$. In the FEM context, this step is usually a computationally expensive step in solving scattering problems, so reusing an LU -decomposition can significantly reduce computational costs. In a second step, the partial derivatives of the system matrix, $\partial A / \partial p_i$, and of the source term, $\partial \mathbf{f} / \partial p_i$, are obtained quasi-analytically, i.e., with negligible computational effort. Then, $A = LU$, \mathbf{E} , $\partial A / \partial p_i$, and $\partial \mathbf{f} / \partial p_i$ are used to compute $\partial \mathbf{E} / \partial p_i$ in Eq. (5). The LU -decomposition can be used to obtain both \mathbf{E} and $\partial \mathbf{E} / \partial p_i$.

For the calculation of the contour integrals, a numerical integration with a circular integration contour and a trapezoidal rule is used, which leads to an exponential convergence behavior with respect to the integration points³¹. At each integration point, we calculate \mathbf{E} and $\partial \mathbf{E} / \partial p_i$ by solving Eq. (1) with oblique incident plane waves as source terms. The linear functional $\mathcal{L}(\mathbf{E})$ corresponds to a spatial point evaluation of one component of the electric field, which can be understood as physical observable. Note that, with Eqs. (3) and (4), an eigenfrequency $\tilde{\omega}$ and its

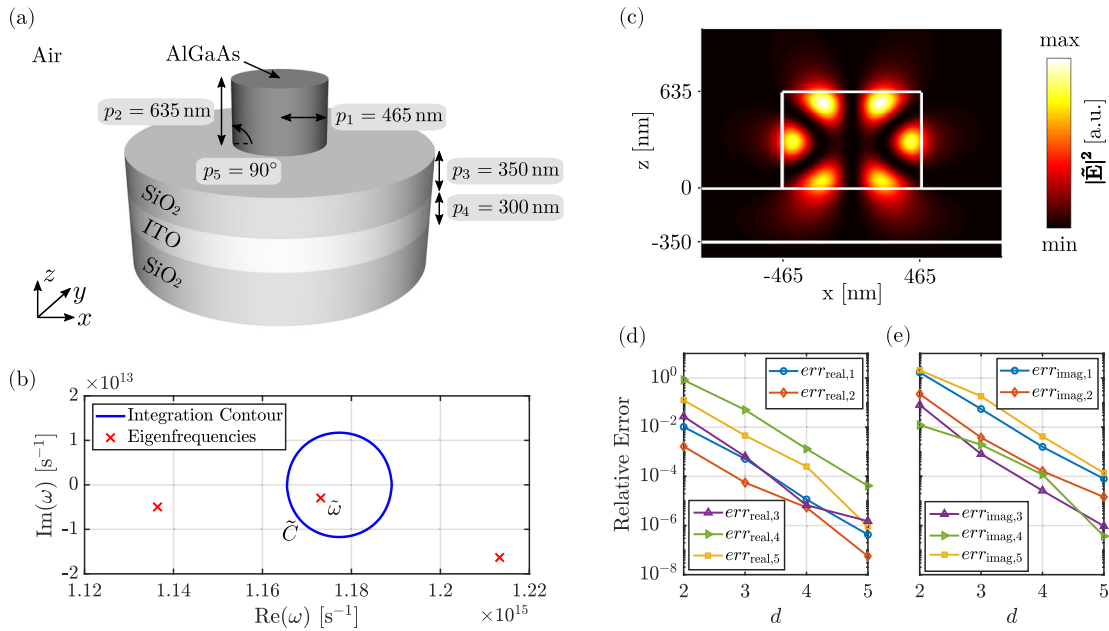


Fig. 2 Numerical investigation of the high-Q resonance of a nanophotonic resonator. **a** Nanoresonator on a three-layer substrate. The substrate is infinitely extended in x and y direction. The geometrical parameters p_1, p_2, \dots, p_5 are the reference values from Koshelev et al.³² **b** Calculated eigenfrequency $\tilde{\omega} = (1.17309 - 0.00296i) \times 10^{15} \text{ s}^{-1}$ corresponding to the high-Q resonance. The other red crosses shown are the two eigenfrequencies which are closest to $\tilde{\omega}$. The circular integration contour \tilde{C} with the center $\omega_0 = 2\pi c/(1600 \text{ nm})$ and the radius $r_0 = \omega_0 \times 10^{-2}$ is used for computing Riesz projections. **c** Electric field intensity $|\tilde{\mathbf{E}}|^2$ corresponding to the high-Q resonance. **d** Convergence of the eigenfrequency sensitivities $\partial\tilde{\omega}/\partial p_i$ with respect to the polynomial degree d of the FEM ansatz functions. The sensitivities are computed at the parameter reference values given in (a). Relative errors $\text{err}_{\text{real},i} = |\text{Re}(\frac{\partial\tilde{\omega}}{\partial p_i}(d) - \frac{\partial\tilde{\omega}}{\partial p_i}(d_{\text{ref}}))|/|\text{Re}(\frac{\partial\tilde{\omega}}{\partial p_i}(d_{\text{ref}}))|$, where $d_{\text{ref}} = 6$. **e** Relative errors $\text{err}_{\text{imag},i}$ for the imaginary parts of the sensitivities; cf. (d).

sensitivity $\partial\tilde{\omega}/\partial p_i$ can be calculated without solving resonance problems $\nabla \times \mu^{-1} \nabla \times \tilde{\mathbf{E}} - \tilde{\omega}^2 \epsilon \tilde{\mathbf{E}} = 0$ directly. Instead, scattering problems, where Eq. (5) can be exploited, are solved. We call the described approach, which combines Riesz projections and direct differentiation (DD), the *Riesz projection DD method*. Equation (4) and its numerical implementation exploiting Eq. (5) are the main results of this work and represent the difference from previous works on Riesz projections; cf. Zschiedrich et al.²⁶

Note that the Riesz projection DD method is not limited to the field of nanophotonics, but can be applied to other eigenproblems as well. Maxwell's equations can be replaced by another partial differential equation, and then instead of the analytical continuation of the electric field \mathbf{E} , the analytical continuation of another quantity is evaluated for the contour integration.

Application

Eigenfrequency sensitivities of a nanophotonic resonator. We investigate an example from the literature, a dielectric nanoresonator of cylindrical shape placed on a three-layer substrate, where constructive and destructive eigenmode interference has been used to engineer a bound state in the continuum (BIC)³². The nanoresonator has been designed taking into account various parameters to suppress radiation losses: The radius, the layer thicknesses, and the layer materials have been chosen to obtain a high-Q resonance. The nanoresonator is made of the high-index material aluminum gallium arsenide (AlGaAs) with 20% aluminum. A silicon dioxide (SiO_2) spacer is placed between the nanoresonator and a film of indium tin oxide (ITO) on a SiO_2 substrate. A sketch of the designed system is shown in Fig. 2a. For this specific configuration, a high-Q resonance with a Q-factor of $Q = 188 \pm 5$ has been experimentally observed, and numerical simulations have resulted in $Q = 197$, where the real part of the resonance wavelength is in the telecommunication wavelength

regime, close to 1600 nm. The nanophotonic resonator has been exploited as a nanoantenna for nonlinear nanophotonics³².

In the following simulations, we consider the constant relative permittivities $\epsilon_r = 10.81$ and $\epsilon_r = 2.084$ for AlGaAs and for SiO_2 , respectively, which are extracted from experimental data^{32,33}. For the ITO layer, the Drude model $\epsilon_r(\omega) = \epsilon_{\text{inf}} - \omega_p^2/(\omega_0^2 + i\omega_0\gamma)$ is chosen, where $\epsilon_{\text{inf}} = 3.8813$, $\omega_p = 3.0305 \times 10^{15} \text{ s}^{-1}$, and $\gamma = 1.2781 \times 10^{14} \text{ s}^{-1}$. This Drude model is obtained by a rational fit³⁴ to experimental data³² and describes the material dispersion of the system. We further exploit the rotational symmetry of the geometry. On the one hand, this reduces the computational effort and, on the other hand, the eigenmodes can be easily distinguished by their azimuthal quantum numbers m , which correspond to the number of oscillations in the radial and axial directions. When the light sources used for computing Riesz projections are not rotationally symmetric, such as oblique incident plane waves, the source fields can be expanded into Fourier modes in the angular direction. Considering Fourier modes with certain quantum numbers, only the eigenmodes, eigenfrequencies, and corresponding sensitivities associated with these quantum numbers are accessed.

We start with computing a Riesz projection to obtain the eigenfrequency $\tilde{\omega}$ of the high-Q resonance. Figure 2b shows the complex frequency plane with the calculated eigenfrequency, $\tilde{\omega} = (1.17309 - 0.00296i) \times 10^{15} \text{ s}^{-1}$, and the corresponding circular integration contour \tilde{C} for the computation of the Riesz projection. The center and the radius of the contour are selected based on a-priori knowledge from Koshelev et al.³². Alternatively, without a-priori knowledge, a larger integration contour can be used²⁵. The simulations are performed using eight integration points on the contour \tilde{C} , where a sufficient accuracy with respect to the integration points is ensured. The computations are based on a FEM mesh consisting of 306 triangles. To compare the size of the contour with the distances between the eigenfrequencies

Table 1 Computed eigenfrequency sensitivities.

i	$\text{Re}(\partial\tilde{\omega}/\partial p_i) \times 10^{-10}$	$\text{Im}(\partial\tilde{\omega}/\partial p_i) \times 10^{-10}$
1	$-128.750 \text{ (s nm)}^{-1}$	$-0.324 \text{ (s nm)}^{-1}$
2	$-84.568 \text{ (s nm)}^{-1}$	$2.660 \text{ (s nm)}^{-1}$
3	$-7.192 \text{ (s nm)}^{-1}$	$-1.955 \text{ (s nm)}^{-1}$
4	$-0.065 \text{ (s nm)}^{-1}$	$0.208 \text{ (s nm)}^{-1}$
5	$15.047 \text{ (s deg)}^{-1}$	$0.039 \text{ (s deg)}^{-1}$

The sensitivities $\partial\tilde{\omega}/\partial p_i$ correspond to the high- Q resonance of the nanoresonator shown in Fig. 2a and are computed at the shown parameter reference values.

within the spectrum of the nanoresonator, the two eigenfrequencies which are closest to $\tilde{\omega}$ are also shown. We obtain a Q -factor of $Q = 198$ for the high- Q resonance, which is in good agreement with the experimental and numerical results from Koshelev et al.³². The corresponding electric field intensity $|\tilde{\mathbf{E}}|^2$ is shown in Fig. 2c. The eigenmode $\tilde{\mathbf{E}}$ has the quantum number $m = 0$ and is strongly localized in the vicinity of the nanoresonator.

Next, the eigenfrequency sensitivities $\partial\tilde{\omega}/\partial p_i$ with respect to the parameters p_1, p_2, \dots, p_5 sketched in Fig. 2a are computed. In order to validate the approach, a convergence study for the polynomial degree d of the FEM ansatz functions is performed. Figure 2d, e shows the relative errors for the real and imaginary parts, respectively. Exponential convergence can be observed for all sensitivities with increasing d . The computed sensitivities for $d = 5$ are shown in Table 1. Exemplary source code for the Riesz projection DD method and simulation results are presented in Binkowski et al.³⁵.

Performance benchmark. The computational effort of the numerical realization of the Riesz projection DD method is compared with the computational effort of the finite difference method. We choose the central difference scheme $\partial\tilde{\omega}/\partial p_i \approx (\tilde{\omega}(p_i + \delta p_i) - \tilde{\omega}(p_i - \delta p_i)) / (2\delta p_i)$ for the comparison. Computing central differences is more computationally expensive than computing forward or backward differences. However, more accurate results can be achieved as the error decreases with $(\delta p_i)^2$. To achieve an adequate accuracy, sufficiently small step sizes δp_i are selected. For example, for the radius of the nanoresonator, we choose $\delta p_1 = 0.1 \text{ nm}$. Note that, also for the finite difference method, we compute the eigenfrequencies by using the contour-integral-based formula in Eq. (3).

We increase the degrees of freedom of the system shown in Fig. 2a by deforming the cylindrical nanoresonator to an ellipsoidal nanoresonator. This breaks the rotational symmetry yielding a full three-dimensional system with new parameters, the radius of the nanoresonator in x direction and the radius in y direction. Figure 3 shows, for the three-dimensional implementation and for the rotational symmetric implementation, the normalized computational effort for different numbers of computed sensitivities. We compute the eigenfrequency $\tilde{\omega}$ and then we add the sensitivities, starting with $\partial\tilde{\omega}/\partial p_1$, one after the other. It can be observed that the Riesz projection DD method requires less computational effort than the finite difference method, for any number of computed sensitivities, i.e., for all $N \geq 1$. In the case of using finite differences, the computational effort has a slope of about 200% because for each sensitivity two additional problems with typically the same dimension as the unperturbed problem have to be solved. In the three-dimensional case, a linear regression for the computational effort gives a slope of about 4% for the Riesz projection DD method. The computational effort needed for the LU -decomposition is significant compared to the matrix assembly and to the other solution steps, so the possibility of exploiting Eq. (5) gives a great benefit for the Riesz projection DD method. For $N = 5$, the CPU

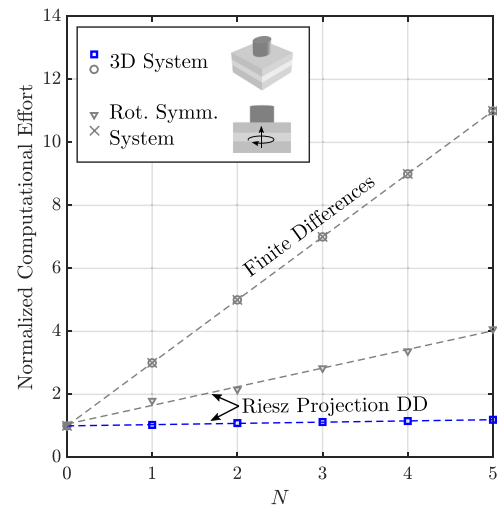


Fig. 3 Performance of the Riesz projection DD method. The normalized computational effort over the number N of computed sensitivities $\partial\tilde{\omega}/\partial p_i$ with respect to parameters p_1, p_2, \dots, p_N is shown. The sensitivities are computed at the reference values shown in Fig. 2a. The computational effort is the total CPU time normalized to the CPU time spent for computing the eigenfrequency $\tilde{\omega}$, which corresponds to $N = 0$. The time is measured with JCMSUITE using four threads on a machine with a 24-core Intel Xeon Processor running at 3.3 GHz. For all calculations, to ensure high accuracies, eight integration points at the integration contour \tilde{C} depicted in Fig. 2b are used. The degree of the FEM ansatz functions is fixed with $d = 5$. The mesh of the three-dimensional system consists of 4160 prisms and the mesh of the rotational symmetric system consists of 306 triangles.

time required to solve the linear system of equations, which includes the LU -decomposition, takes 81% of the accumulated CPU time. In the rotational symmetric case, the time for solving the linear system is negligible. However, the trend is the same for the three-dimensional and for the computationally cheaper rotational symmetric case: The advantage of using Riesz projections significantly increases with an increasing number of computed sensitivities.

Note that contour integral methods are well suited for parallelization because the scattering problems can be solved in parallel on the integration contour. However, as total CPU times are considered for Fig. 3, this is not reflected by the time measurements.

Q -factor optimization. The Riesz projection DD method is applied to further optimize the Q -factor of the high- Q resonance of the nanophotonic resonator from Koshelev et al.³² shown in Fig. 2a. A rotational symmetric nanoresonator is considered because simulations show that an ellipsoidal shape does not lead to a significant increase of the Q -factor. We use a Bayesian optimization algorithm³⁶ with the incorporation of sensitivity information. This global optimization algorithm is well suited for problems with computationally expensive objective functions and benchmarks show that providing sensitivities can significantly reduce computational effort³⁷. However, other optimization approaches could be used as well.

For the optimization, we choose the parameter ranges $435 \text{ nm} \leq p_1 \leq 495 \text{ nm}$, $575 \text{ nm} \leq p_2 \leq 695 \text{ nm}$, $150 \text{ nm} \leq p_3 \leq 550 \text{ nm}$, $100 \text{ nm} \leq p_4 \leq 500 \text{ nm}$, and $60^\circ \leq p_5 \leq 90^\circ$. To ensure that the optimized nanoresonator can also be used as nanoantenna in the telecommunication wavelength regime, like the original system, we add the constraint that the optimized eigenfrequency must lie in the circular contour with the center $\omega_0 = 2\pi c/(1600 \text{ nm})$ and the radius $r_0 = 4 \times 10^{13} \text{ s}^{-1}$. In each optimization step, the Riesz

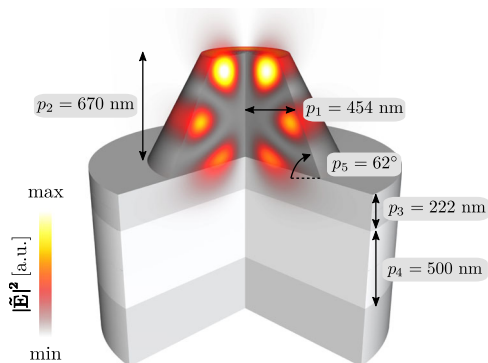


Fig. 4 Optimization of a nanophotonic resonator. The optimized nanophotonic resonator with a sketch of the electric field intensity $|\mathbf{E}|^2$ corresponding to the high-Q resonance is shown. The high-Q resonance has a Q-factor of $Q = 292$. The materials of the nanoresonator are the same as for the reference structure in Fig. 2a.

projection DD method is used to compute the eigenfrequency with a quantum number of $m = 0$ lying inside the contour and to calculate the corresponding sensitivities.

A nanoresonator with a Q-factor of $Q = 292$ is obtained after 61 iterations of the optimizer yielding an increase of about 47.5% over the original resonator. More iterations yield only a negligible increase of the Q-factor. The optimized nanoresonator with a sketch of the electric field intensity of its high-Q resonance and the values for all underlying parameters are shown in Fig. 4. The corresponding eigenfrequency is given by $\tilde{\omega}_{\text{opt}} = (1.176897 - 0.002015i) \times 10^{15} \text{ s}^{-1}$. Note that, in the optimization domain, the average sensitivity of the Q-factor with respect to the ITO layer thickness p_4 is negligible.

Conclusions

An approach for computing eigenfrequency sensitivities of resonance problems was presented. The numerical realization of the Riesz projection DD method relies on computing scattering solutions and their sensitivities by solving Maxwell's equations with a source term, i.e., solving linear systems of equations. This enables direct differentiation for the efficient calculation of eigenfrequency sensitivities. Although sensitivities of resonances are computed, no eigenproblems have to be solved directly. The performance of the approach was demonstrated by a comparison with the finite difference method. The Riesz projection DD method was incorporated into a gradient-based optimization algorithm to maximize the Q-factor of a nanophotonic resonator.

The savings in computational effort are particularly significant for optimization with respect to several parameters, which is a common task in nanophotonics. Therefore, we expect the approach to prove especially useful when many sensitivities are to be calculated. The Riesz projection DD method can not only be applied to problems in nanophotonics, but to any resonance problem.

Data availability

All relevant data generated or analyzed during this study are included in this published article. Tabulated data files are included in a corresponding data publication³⁵.

Code availability

Source code for performing the numerical experiments can be found in Binkowski et al.³⁵.

Received: 7 April 2022; Accepted: 19 July 2022;

Published online: 10 August 2022

References

- Novotny, L. & van Hulst, N. Antennas for light. *Nat. Photonics* **5**, 83–90 (2011).
- Kuznetsov, A. I., Miroshnichenko, A. E., Brongersma, M. L., Kivshar, Y. S. & Luk'yanchuk, B. Optically resonant dielectric nanostructures. *Science* **354**, aag2472 (2016).
- Senellart, P., Solomon, G. & White, A. High-performance semiconductor quantum-dot single-photon sources. *Nat. Nanotechnol.* **12**, 1026–1039 (2017).
- Anker, J. N. et al. Biosensing with plasmonic nanosensors. *Nat. Mater.* **7**, 442–453 (2008).
- Ma, R.-M. & Oulton, R. F. Applications of nanolasers. *Nat. Nanotechnol.* **14**, 12–22 (2019).
- Ma, X.-C., Dai, Y., Yu, L. & Huang, B.-B. Energy transfer in plasmonic photocatalytic composites. *Light Sci. Appl.* **5**, e16017 (2016).
- Zhang, Y. et al. Surface-plasmon-driven hot electron photochemistry. *Chem. Rev.* **118**, 2927–2954 (2018).
- Lalanne, P. et al. Light interaction with photonic and plasmonic resonances. *Laser Photonics Rev.* **12**, 1700113 (2018).
- Wu, T., Gurioli, M. & Lalanne, P. Nanoscale light confinement: The Q's and V's. *ACS Photonics* **8**, 1522–1538 (2021).
- West, P. R. et al. Searching for better plasmonic materials. *Laser Photonics Rev.* **4**, 795–808 (2010).
- Wang, B. et al. High-Q plasmonic resonances: Fundamentals and applications. *Adv. Opt. Mater.* **9**, 2001520 (2021).
- Lalanne, P. et al. Quasinormal mode solvers for resonators with dispersive materials. *J. Opt. Soc. Am. A* **36**, 686–704 (2019).
- Bindel, D. & Hood, A. Localization theorems for nonlinear eigenvalue problems. *SIAM J. Matrix Anal. Appl.* **34**, 1728–1749 (2013).
- Güttel, S. & Tisseur, F. The nonlinear eigenvalue problem. *Acta Numer.* **26**, 1–94 (2017).
- Jensen, J. S. & Sigmund, O. Topology optimization for nano-photonics. *Laser Photonics Rev.* **5**, 308–321 (2011).
- Bouhelle, M. A. et al. A python surrogate modeling framework with derivatives. *Adv. Eng. Softw.* **135**, 102662 (2019).
- Cacuci, D. G., Ionescu-Bujor, M. & Navon, I. M. *Sensitivity and Uncertainty Analysis, Volume II: Applications to Large-Scale Systems* 1st edn (CRC Press, 2005).
- Kato, T. *Perturbation Theory for Linear Operators* 2nd edn (Springer-Verlag, 1995).
- Sakurai, J. J. & Napolitano, J. *Modern Quantum Mechanics* 3rd edn (Cambridge University Press, 2020).
- Burschäpers, N., Fiege, S., Schuhmann, R. & Walther, A. Sensitivity analysis of waveguide eigenvalue problems. *Adv. Radio Sci.* **9**, 85–89 (2011).
- Swillam, M. A., Bakr, M. H., Li, X. & Deen, M. J. Efficient sensitivity analysis of the time independent Schrödinger equation with application to quantum lasers. *Opt. Commun.* **281**, 4459–4463 (2008).
- Yan, W., Lalanne, P. & Qiu, M. Shape deformation of nanoresonator: A quasinormal-mode perturbation theory. *Phys. Rev. Lett.* **125**, 013901 (2020).
- Alam, R. & Safique Ahmad, S. K. Sensitivity analysis of nonlinear eigenproblems. *SIAM J. Matrix Anal. Appl.* **40**, 672–695 (2019).
- Binkowski, F., Zschiedrich, L. & Burger, S. A Riesz-projection-based method for nonlinear eigenvalue problems. *J. Comput. Phys.* **419**, 109678 (2020).
- Betz, F., Binkowski, F. & Burger, S. RPEExpand: Software for Riesz projection expansion of resonance phenomena. *SoftwareX* **15**, 100763 (2021).
- Zschiedrich, L. et al. Riesz-projection-based theory of light-matter interaction in dispersive nanoresonators. *Phys. Rev. A* **98**, 043806 (2018).
- Pomplun, J., Burger, S., Zschiedrich, L. & Schmidt, F. Adaptive finite element method for simulation of optical nano structures. *Phys. Status Solidi B* **244**, 3419–3434 (2007).
- Hohenester, U. & Trügler, A. MNPBEM—A Matlab toolbox for the simulation of plasmonic nanoparticles. *Comput. Phys. Commun.* **183**, 370–381 (2012).
- Nikolova, N. K., Bandler, J. W. & Bakr, M. H. Adjoint techniques for sensitivity analysis in high-frequency structure CAD. *IEEE Trans. Microw. Theory Technol.* **52**, 403–419 (2004).
- Burger, S., Zschiedrich, L., Pomplun, J., Schmidt, F. & Bodermann, B. Fast simulation method for parameter reconstruction in optical metrology. *Proc. SPIE* **8681**, 380–386 (2013).
- Trefethen, L. N. & Weideman, J. A. C. The exponentially convergent trapezoidal rule. *SIAM Rev.* **56**, 385–458 (2014).
- Koshelev, K. et al. Subwavelength dielectric resonators for nonlinear nanophotonics. *Science* **367**, 288–292 (2020).
- Malitson, I. H. Interspecimen comparison of the refractive index of fused silica. *J. Opt. Soc. Am.* **55**, 1205–1209 (1965).
- Sehmi, H. S., Langbein, W. & Muljarov, E. A. Optimizing the Drude-Lorentz model for material permittivity: Method, program, and examples for gold, silver, and copper. *Phys. Rev. B* **95**, 115444 (2017).
- Binkowski, F. et al. Source code and simulation results for Computation of eigenfrequency sensitivities using Riesz projections for efficient optimization of nanophotonic resonators. Zenodo <https://doi.org/10.5281/zenodo.6614951> (2022).

36. Pelikan, M., Goldberg, D. E. & Cantú-Paz, E. BOA: The Bayesian optimization algorithm. *GECCO'99: Proc. Gen. Ev. Comp. Conf.* **1**, 525 (1999).
37. Schneider, P.-I. et al. Benchmarking five global optimization approaches for nano-optical shape optimization and parameter reconstruction. *ACS Photonics* **6**, 2726–2733 (2019).

Acknowledgements

We acknowledge funding by the Deutsche Forschungsgemeinschaft (DFG, German Research Foundation) under Germany's Excellence Strategy - The Berlin Mathematics Research Center MATH+ (EXC-2046/1, project ID: 390685689) and the German Federal Ministry of Education and Research (BMBF Forschungscampus MODAL, project 05M20ZBM). This project has received funding from the EMPIR program co-financed by the Participating States and from the European Union's Horizon 2020 research and innovation program (project 20FUN02 POLIGHT). We further thank Kirill Koshelev for providing the experimental material data for the physical system investigated in this work.

Author contributions

F.Bi., L.Z., and S.B. conceived and designed the research; F.Bi. and F.Be. performed the numerical simulations with input from M.H. and P.-I.S.; All authors discussed the results; F.Bi. wrote the manuscript with input from all authors.

Funding

Open Access funding enabled and organized by Projekt DEAL.

Competing interests

The authors declare no competing interests.

Additional information

Supplementary information The online version contains supplementary material available at <https://doi.org/10.1038/s42005-022-00977-1>.

Correspondence and requests for materials should be addressed to Sven Burger.

Peer review information *Communications Physics* thanks Zhiyuan Fan and the other anonymous reviewer(s) for their contribution to the peer review of this work. Peer reviewer reports are available.

Reprints and permission information is available at <http://www.nature.com/reprints>

Publisher's note Springer Nature remains neutral with regard to jurisdictional claims in published maps and institutional affiliations.



Open Access This article is licensed under a Creative Commons Attribution 4.0 International License, which permits use, sharing, adaptation, distribution and reproduction in any medium or format, as long as you give appropriate credit to the original author(s) and the source, provide a link to the Creative Commons license, and indicate if changes were made. The images or other third party material in this article are included in the article's Creative Commons license, unless indicated otherwise in a credit line to the material. If material is not included in the article's Creative Commons license and your intended use is not permitted by statutory regulation or exceeds the permitted use, you will need to obtain permission directly from the copyright holder. To view a copy of this license, visit <http://creativecommons.org/licenses/by/4.0/>.

© The Author(s) 2022